arXiv:cond-mat/0008084v1 [cond-mat.mtrl-sci] 5 Aug 2000

Thermal conductivity of amorphous carbon thin films

Andrew J. Bullen, Keith E. O'Hara, and David G. Cahill
Department of Materials Science and Engineering, Coordinated Science Laboratory, and Materials Research Laboratory, University of Illinois, Urbana, Illinois 61801

Othon Monteiro
Lawrence Berkeley Laboratory, University of California, Berkeley, CA 94720

Achim von Keudell
Max-Planck-Intitut für Plasmaphysik, D-85740 Garching bei München, Germany
(February 1, 2008)

Thermal conductivities Λ of amorphous carbon thin films are measured in the temperatures range 80–400 K using the 3ω method. Sample films range from soft a-C:H prepared by remote-plasma deposition ($\Lambda = 0.20$ W m^{-1} K^{-1} at room temperature) to amorphous diamond with a large fraction of sp^3 bonded carbon deposited from a filtered-arc source ($\Lambda = 2.2$ W m^{-1} K^{-1}). Effective-medium theory provides a phenomenological description of the variation of conductivity with mass density. The thermal conductivities are in good agreement with the minimum thermal conductivity calculated from the measured atomic density and longitudinal speed of sound.

I. INTRODUCTION

Amorphous carbon (a-C) exists in an amazing variety of forms with microstructures and physical properties that depend sensitively on preparation method [1]. Because a-C thin films are often used as protective coatings, the most thoroughly studied of these structure-property relationships are the dependence of the mechanical properties, e.g., elastic constants and hardness, on deposition conditions, atomic density, and hydrogen content. The focus of our experimental study, thermal conductivity, like the mechanical properties, derives from the bonding and geometry of the atomic lattice. The large variability of microstructures within this single class of materials provides a unique opportunity for exploring heat transport in disordered solids [2,3] and the applicability of the minimum thermal conductivity [4,5] to materials with heterogeneous microstructures that are common in thin films [6,7]. But we also anticipate that these new data will provide valuable insights on the high and low conductivities that can be produced in thin film a-C for applications in the thermal engineering of micro-devices [8,9].

The concept of a "minimum thermal conductivity" $\Lambda_{\rm min}$ is based on a theory of heat transport originally proposed by Einstein [10]: the atomic vibrations are assumed to be incoherent and therefore heat diffuses between the Einstein oscillators on a time scale of $1/2$ the period of vibration. Einstein's theory could not explain the large thermal conductivities of most crystalline dielectrics but his and related models [4,5,11] are useful for understanding the thermal conductivity of amorphous materials and crystals with certain types of strong disorder.

We include larger oscillating entities than the single atoms considered by Einstein by borrowing from the Debye model of lattice vibrations and dividing the sample into regions of size $\lambda/2$, where λ is an acoustic wavelength, and whose frequencies of oscillation are given by the low frequency speed of sound $\omega = 2\pi v/\lambda$ [5,7].

$$\Lambda_{\min} = \left(\frac{\pi}{6}\right)^{1/3} k_B n^{2/3} \sum_{i=1}^{3} v_i \left(\frac{T}{\Theta_i}\right)^2 \int_0^{\Theta_i/T} \frac{x^3 e^x}{(e^x-1)^2} dx \quad . \tag{1}$$

The index i labels the three sound modes (two transverse and one longitudinal) with speeds of sound v_i; Θ_i is the cutoff frequency for each polarization expressed in degrees K, $\Theta_i = v_i(\hbar/k_B)(6\pi^2 n)^{1/3}$, and n is the number density of atoms. This model has no free parameters and is in good agreement with data for a wide variety of bulk disordered materials near room temperature [5].

Since diamond has the largest values of n and v_i [12] of any material, the high temperature limit of $\Lambda_{\min}$ also has the largest possible value. Figure 1 shows the calculated $\Lambda_{\min}$ for diamond with comparisons to previously published data for amorphous carbon [7,13–15]. Data for bulk samples of high-dose neutron-irradiated diamond [13] and disordered carbon produced by high-pressure conversion of C_{60} [15] were measured by traditional steady-state methods; the conductivities of thin film samples were measured using the mirage effect [14] and picosecond thermoreflectance [7]. The thin film data were measured only for room temperature, and therefore the unusual temperature of the two bulk samples cannot be confirmed in the thin film samples. Furthermore, while picosecond reflectance is a powerful probe of elastic properties and interfacial transport of acoustic and thermal energy, measurements of thermal conductivity using this method are relatively indirect and require assumptions about the heat capacity of the films [7].

II. EXPERIMENTAL DETAILS

Thin film samples of a-C:H were prepared at the Max-Planck-Institut für Plasmaphysik by remote-plasma chemical vapor deposition (RPCVD)—chosen to produce a soft, low-density form of a-C:H—and by plasma-assisted CVD (PACVD); the PACVD samples have mechanical properties that are typical for protective coatings of "diamond-like-carbon" (DLC) [16]. Carbon-to-hydrogen ratios measured on similar samples are 1:1 for RPCVD and 2:1 for PACVD. Additional samples of DLC films were obtained from Delphi Automotive Systems and Surmet Corporation. At Lawrence Berkeley Laboratory, a-C films were deposited by filtered-arc deposition (FAD) [17–19] using two acceleration voltages, 100 and 2000 V. The fractions of sp^3 bonded carbon measured by EELS [18] on similar samples are 80% at 100 V bias and 30% at 2000 V bias; a-C films with low concentrations of hydrogen and carbon bonding dominated by sp^3 hybridization are often referred to as "amorphous diamond" (a-D) or "tetrahedrally-bonded" amorphous carbon (ta-C).

We use the 3ω method [20,21] to measure the thermal conductivity of a-C films in the temperature range $80 < T < 400$ K. A 10 μm wide Al line—sputter deposited on the surface of the sample and patterned by photolithography—serves as both the heater and the thermometer in the measurement. If the film thickness h is small compared to the width of the metal line, heat flow is one-dimensional in the thin film and two-dimensional (radial) in the substrate [21]. Also, as long as h is small compared to the penetration depth of the thermal waves, the thin film simply adds a frequency-independent temperature oscillation to the known thermal response of the substrate. Most of our a-C samples were deposited on Si substrates with a 100 nm thick layer of thermally grown SiO_2 which is needed to improve the electrical isolation between the Si substrates and the Al metallization. The added thermal resistance of the SiO_2 layer is measured separately and subtracted from the raw data [21].

Conversion of the measured thermal resistance to thermal conductivity requires accurate measurements of film thickness h. We measure h using spectroscopic variable-angle ellipsometry; the optical properties of the a-C films are modeled using a fit to the resonant frequency, oscillator strength, and damping of two Lorentz-oscillators. Alternatively, e.g., if the optical modeling produced a poor fit to the ellipsometry data, we use scanning electron microscopy of a fracture cross-section to measure h. Areal densities of carbon are measured using Rutherford backscattering spectrometry of the stopping power of the a-C film. The combination of areal density and h gives the film density, see Table I. We measure longitudinal speeds of sound v_l by "picosecond ultrasonics" [7]: an Al thin-film transducer produces and detects acoustic waves generated by a mode-locked Ti:sapphire laser operating at 780 nm; values for v_l are listed in Table I.

III. RESULTS AND DISCUSSION

Figure 2 shows the results of our thermal conductivity measurements. In all cases, the thermal conductivity has the temperature dependence expected for an amorphous solid in this temperature range [5]. In four cases, we measured the same type of film for two values of the thickness h to determine the effects of the finite thermal conductance of interfaces on our measurements [21]. For the relatively low conductivities of the RPCVD and PACVD films, see Fig. 2a, the interface effects have little effect on the measured conductivity of films with $h \sim 100$ nm. Interface effects are more pronounced in the FAD films, see Fig. 2b. Using the assumption that the true conductivity of the film is independent of film thickness, we can separate the true conductivity of the film from the interface thermal conductance [21]; for both sets of FAD films shown in Fig. 2b, the true conductivity is $\approx 15\%$ larger than the measured conductivity of the thicker film.

We have discovered that effective medium theory [25] provides a surprisingly good description of the variation of conductivity with mass density [22]. The conductivity of a composite structure made of a matrix material and spherical inclusions of a second phase is given by [25]:

$$4\Lambda = (3f_2 - 1)\Lambda_2 + (3f_1 - 1)\Lambda_1 + \left[((3f_2 - 1)\Lambda_2 + (3f_1 - 1)\Lambda_1)^2 + 8\Lambda_1\Lambda_2\right]^{1/2}, \quad (2)$$

where Λ_1 is the conductivity of the matrix, Λ_2 is the conductivity of the second phase, and f_1, f_2 are the volume fractions of the matrix and second phase, respectively. Figure 3 compares the predictions of this theory to the room temperature conductivity of a-C films. The theory fits the data reasonably well and enables us to extrapolate the conductivity to the full density of diamond, $\Lambda = 4.0$ W m^{-1} K^{-1}.

Experiments on a-C have often been interpreted in terms of heterogeneous microstructures [23,24], but the accuracy and generality of these various microstructural models remains controversial. Our two-component model, see Eq. 2 and Fig. 3, for the thermal conductivity is probably an oversimplification of the true complexity of a-C microstructures. Nevertheless, we believe this phenomenological model will be a useful engineering guide for predicting the conductivity of a-C films when only the density is known.

Figure 2 also includes comparisons of the data to the calculated $\Lambda_{\min}$ for samples A (DLC prepared by PACVD) and H ("amorphous diamond" prepared by FAD). The temperature dependence of $\Lambda_{\min}$ is steeper than the data; this result is generally observed for both bulk [5] and thin film [6] amorphous materials since Eq. 1 does not include contributions to the heat transport by low frequency phonons with long mean-free-paths [3]. But in the high temperature limit, the agreement is good, particularly for sample H, see Fig. 2b.

The agreement between the measured and calculated conductivities is made more explicit in Fig. 4 where we compare the high temperature limit of $\Lambda_{\min}$ to the data at 400 K, the highest temperature of our measurements. (Data for sample L are restricted to $T < 300$ K because of stray electrical conductance at higher temperatures. In this case, we have extrapolated the data to 400 K using the temperature dependence of sample H.) The calculations reproduce the trend in the data well; we note, however, that the calculated conductivities are consistently greater than the measured values. The fact that the thermal conductivities are increasing with temperature contributes to this discrepancy; measurements at higher temperatures would show better agreement with the model. For the lowest conductivity films, however, the temperature dependence of the data is relatively weak and the calculated conductivity exceeds the measured value at 400 K by a factor of ≈ 2. This relatively large difference between measured and calculated conductivity is also observed in amorphous Se [5]. But given the simplifying assumptions of the model [5], disagreements of this magnitude are expected and we conclude that the minimum thermal conductivity calculated from the mean atomic densities and speeds of sound provides an adequate description of heat transport in a wide variety of a-C thin film materials.

IV. ACKNOWLEDGEMENTS

We thank Don Morelli and the Surmet Corp. for providing additional samples of DLC. This work was supported by NSF Grant No. CTS 99-78822. Sample characterization by RBS, SEM, ellipsometry, and picosecond ultrasonics used the facilities of the Center for Microanalysis of Materials, supported by U.S. DOE Grant No. DEFG02-96-ER45439.

[1] J. Robertson, Advances in Physics **35**, 317 (1986); J. Robertson, Progress in Solid State Chemistry **21**, 199 (1991).
[2] R. Orbach, Philos. Mag. B **65**, 289 (1992).
[3] J. L. Feldman, Philip B. Allen, and Scott R. Bickham, Phys. Rev. B **59**, 3551 (1999).
[4] Glen A. Slack, in *Solid State Physics: Advances in Research and Applications*, edited by F. Seitz and A. G. Turnball (Academic, New York, 1979), Vol. 34, p. 1.
[5] David G. Cahill, S. K. Watson, and R. O. Pohl, Phys. Rev. B **46**, 6131 (1992).
[6] S.-M. Lee, David G. Cahill, and Thomas H. Allen, Phys. Rev. B **52**, 253 (1995).
[7] C. J. Morath, H. J. Maris, J. J. Cuomo, D. L. Pappas, A. Grill, V. V. Patel, J. P. Doyle, and K. L. Saenger, J. Appl. Phys. **76**, 2636 (1994).
[8] K. E. Goodson, Y.-S. Ju, and M. Asheghi, in *Microscale Energy Transport,* edited by C. L. Tien, A. Majumdar, and F. M. Gerner, (Taylor & Francis, New York, 1998), pp. 229-293.
[9] Kenneth E. Goodson and Y. Sugtaek Ju, Ann. Rev. Mat. Sci. **29**, 261 (1999).
[10] A. Einstein, Ann. Phys. **35**, 679 (1911).
[11] C. Kittel, Phys. Rev. **75**, 972 (1948).
[12] H. J. McSkimin and W. L. Bond, Phys. Rev. **105**, 116 (1957).
[13] D. T. Morelli, T. A. Perry, J. W. Vandersande, and C. Uher, Phys. Rev. B **48**, 3037 (1993).
[14] W. Hurler, M. Pietralla, A. Hammerschmidt, Diamond & Related Materials **4**, 954 (1995).
[15] A. Smontara, K. Biljakovic, D. Staresinic, D. Pajic, M. E. Kozlov, M. Hirabayashi, M. Tokumoto, H. Ihara, Physica B **219&220**, 160 (1996).
[16] J. W. Zou, K. Reichelt, K. Schmidt, and B. Dischler, J. Appl. Phys. **65**, 3914 (1989).
[17] S. Aisenberg and R. Chabot, J. Appl. Phys. **42**, 2953 (1971).
[18] G. M. Pharr, D. L. Callahan, S. D. McAdams, T.-Y. Tsui, S. Anders, A. Anders, J. W. Ager III, I. G. Brown, C. S. Bhatia, S. R. P. Silva, and J. Robertson, Appl. Phys. Lett. **68**, 779 (1996).
[19] P. J. Fallon, V. S. Veerasamy, C. A. Davis, J. Robertson, G. A. J. Amaratunga, W. I. Milne, and J. Koskinen, Phys. Rev. B **48** 4777 (1993).
[20] David G. Cahill, Rev. Sci. Instrum. **61**, 802 (1990).

[21] S.-M. Lee and David G. Cahill, J. Appl. Phys. **81**, 2590 (1997).
[22] Effective medium theories have often been used for modeling the optical properties of a-C; see, for an early example, F. W. Smith, J. Appl. Phys. **55**, 764 (1984).
[23] J. Robertson and E. P. O'Reilly, Phys. Rev. B **35**, 2946 (1987).
[24] C. Jäger, J. Gottwald, H. W. Spiess, and R. J. Newport, Phys. Rev. B **50**, 846 (1994).
[25] R. Landauer, J. Appl. Phys. **23**, 779 (1952).

FIG. 1. Summary of published data for amorphous carbon with comparison to the minimum thermal conductivity $\Lambda_{\min}$ calculated for diamond (dashed line) and the highest thermal conductivity measured in this work (sample H, filled circles, see description in Table I); i) neutron-D, diamond irradiated by neutrons at 2×10^{22} cm^{-2} Ref. [13]; ii) P-C_{60}, high-pressure conversion of C_{60}, Ref. [15]; iii) DLC, range of conductivities measured in diamond-like carbon thin films at room temperature, Refs. [7] and [14]; iv) a-D, range of conductivities measured in amorphous diamond films at room temperature, Ref. [7].

FIG. 2. Thermal conductivity of a-C films deposited by (a) plasma-assisted chemical vapor deposition, and (b) filtered-arc deposition. Data symbols are labelled by a letter that identifies each sample; see Table I for sample descriptions; $\Lambda_{\min}$ for samples A and H are shown as dashed lines in (a) and (b), respectively.

FIG. 3. Room temperature thermal conductivity of a-C thin films as a function of mass density. The thermal conductivity of the filtered-arc deposited a-C has been adjusted by a small factor ($\approx 15\%$) to correct for the finite interface conductance. The dashed-line is an effective medium calculation (Eq. 2) using two-components; component 1 has the conductivity and density of our lowest conductivity film and component 2 has the density of diamond $\rho = 3.51$ g cm^{-3}. The conductivity of component 2 is adjusted to fit the data: $\Lambda_2 = 4.0$ W m^{-1} K^{-1}.

FIG. 4. Comparison of the thermal conductivity at 400 K for samples C, A, L, and H and the high temperature limit of Eq. 1; $\Lambda_{\min} = 0.40 k_B n^{2/3}(v_l + 2v_t)$. Longitudinal speeds of sounds v_l are measured by picosecond ultrasonics (see Table I); we assume $v_t \approx 0.60 v_l$ (corresponding to a Poisson's ratio of 0.22) and ignore the contribution of hydrogen to the atomic densities n. The dashed line indicates perfect agreement between measured and calculated values.

TABLE I. Deposition parameters and physical properties of a-C films. Films are deposited by plasma-assisted chemical vapor deposition (PACVD), remote-plasma CVD (RPCVD), and filtered-arc deposition (FAD). Films were deposited at the Max-Planck-Institut für Plasmaphysik (A,B,C,D), and Lawrence Berkeley Laboratory (H,I,L,M). Additional samples were obtained from the Surmet Corporation (F,G) and Delphi Automotive Systems (E).

Sample	Film thickness (nm)	Density (g cm^{-3})	v_l km sec^{-1}	Method	Bias (volt)
A,B	94,313	1.8	8.7	PACVD	200
C,D	108,325	0.9	3.4	RPCVD	15
E	3800	2.1	—	PACVD	450
F	120	1.2	—	PACVD	0
G	280	1.7	—	PACVD	0
H,I	475,92	2.8	14.0	FAD	100
L,M	195,65	2.3	12.7	FAD	2000

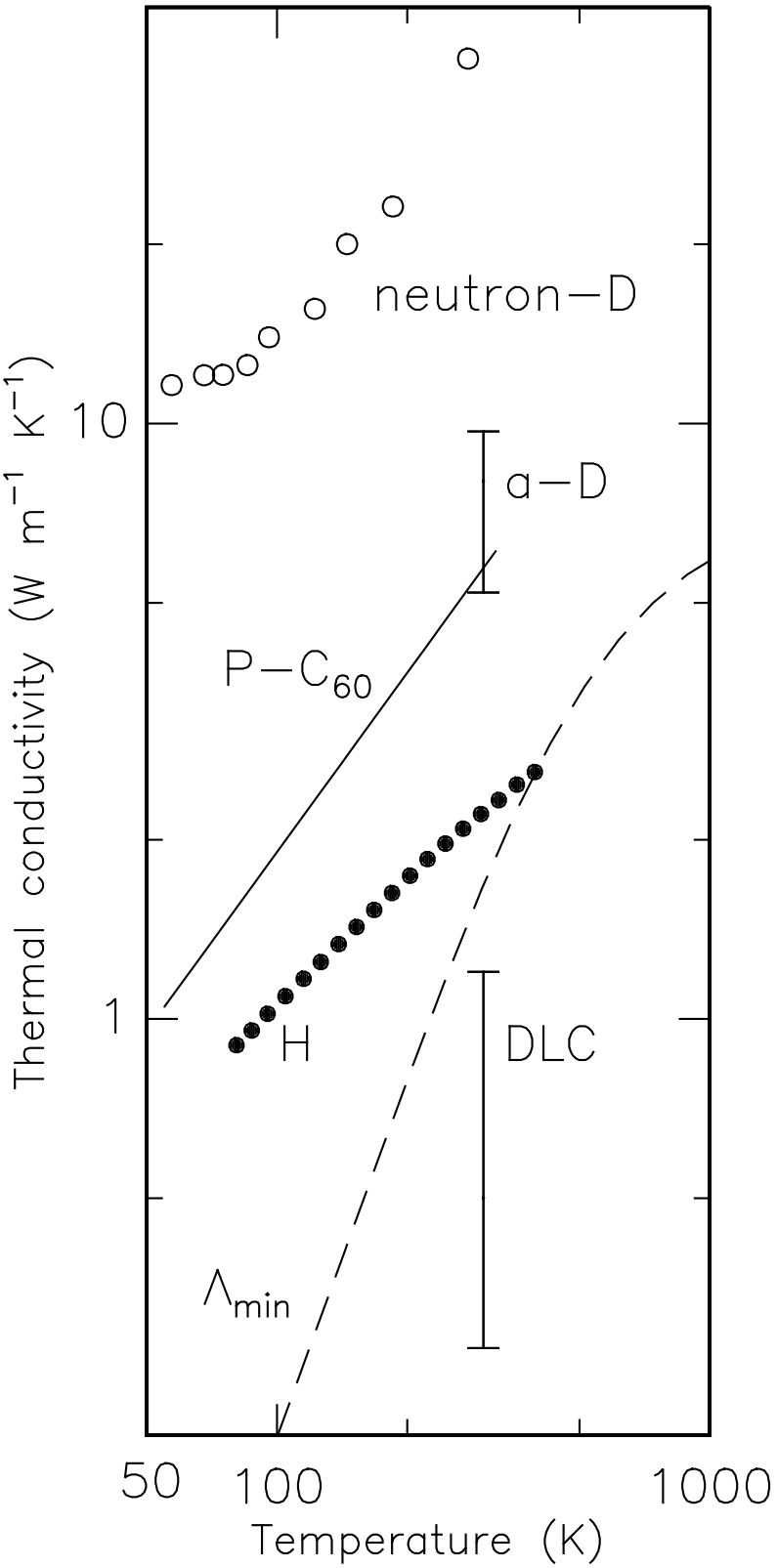
neutron−D
a−D
P−C60
H
DLC
Λmin
10
1
50
100
1000
Thermal conductivity (W m−1 K−1)
Temperature (K)

Figure 1

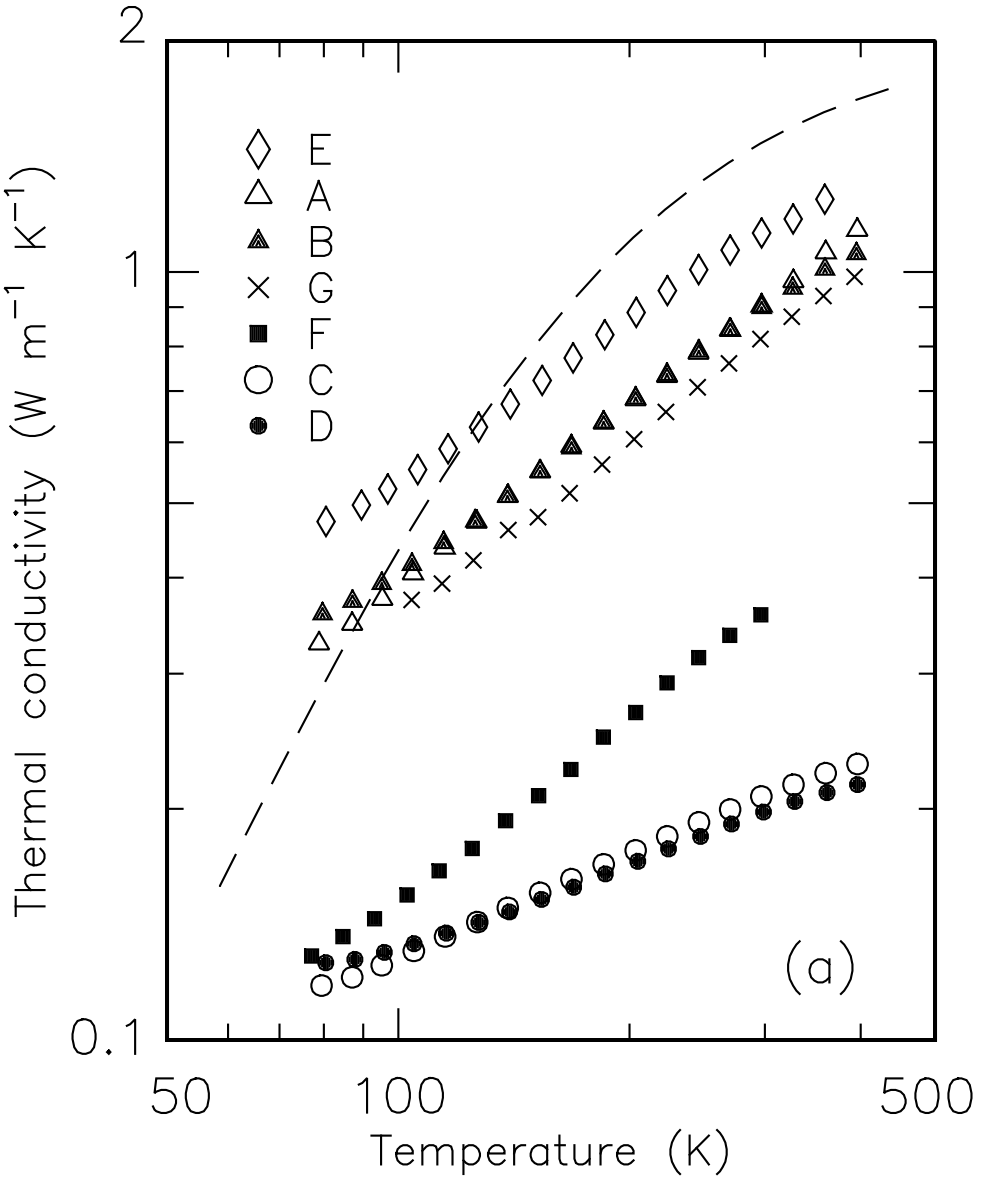
2
1
0.1
50
100
500
Thermal conductivity (W m^{-1} K^{-1})
Temperature (K)
E
A
B
G
F
C
D
(a)

Figure 2a

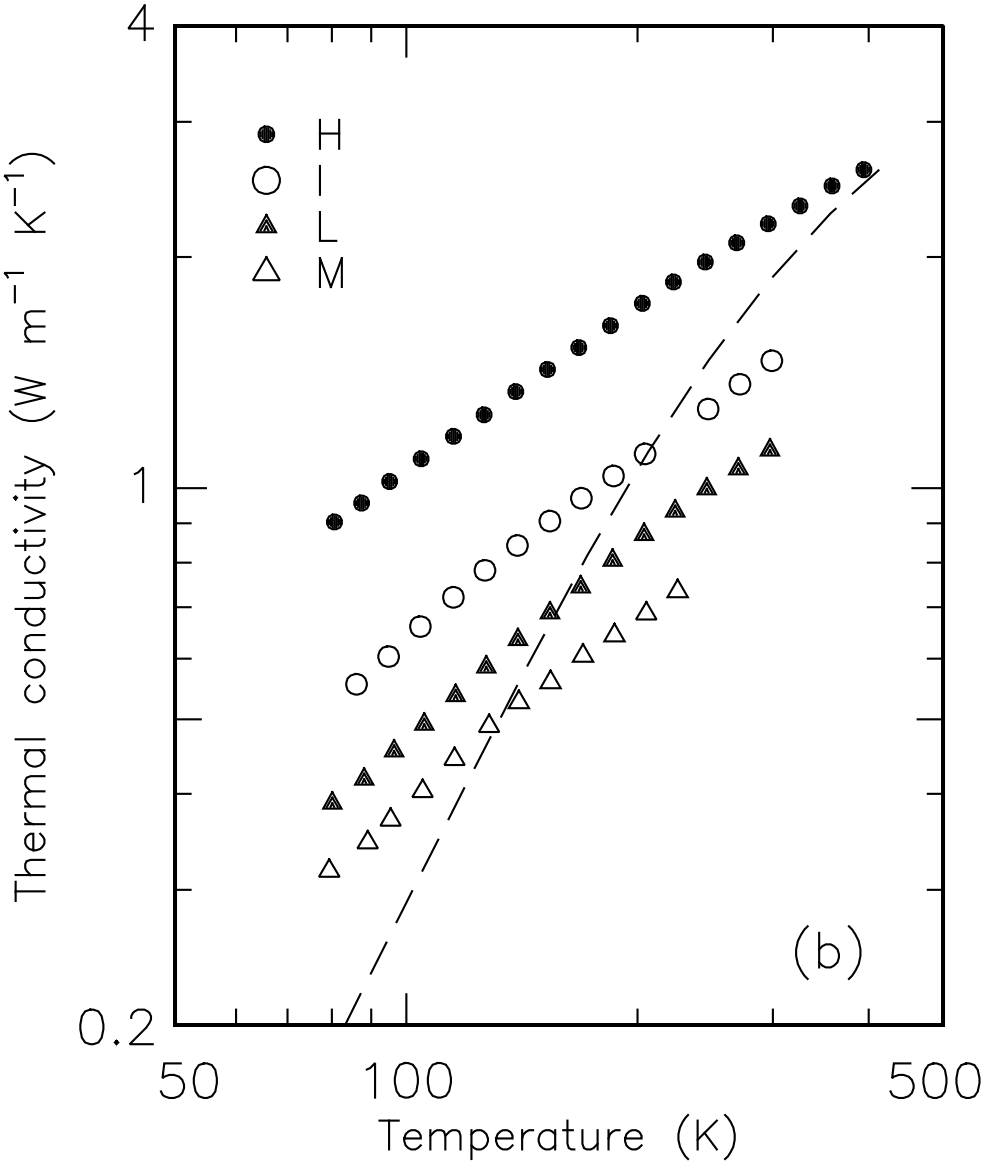
4
1
0.2
50
100
500
Thermal conductivity (W m^{-1} K^{-1})
Temperature (K)
H
I
L
M
(b)

Figure 2b

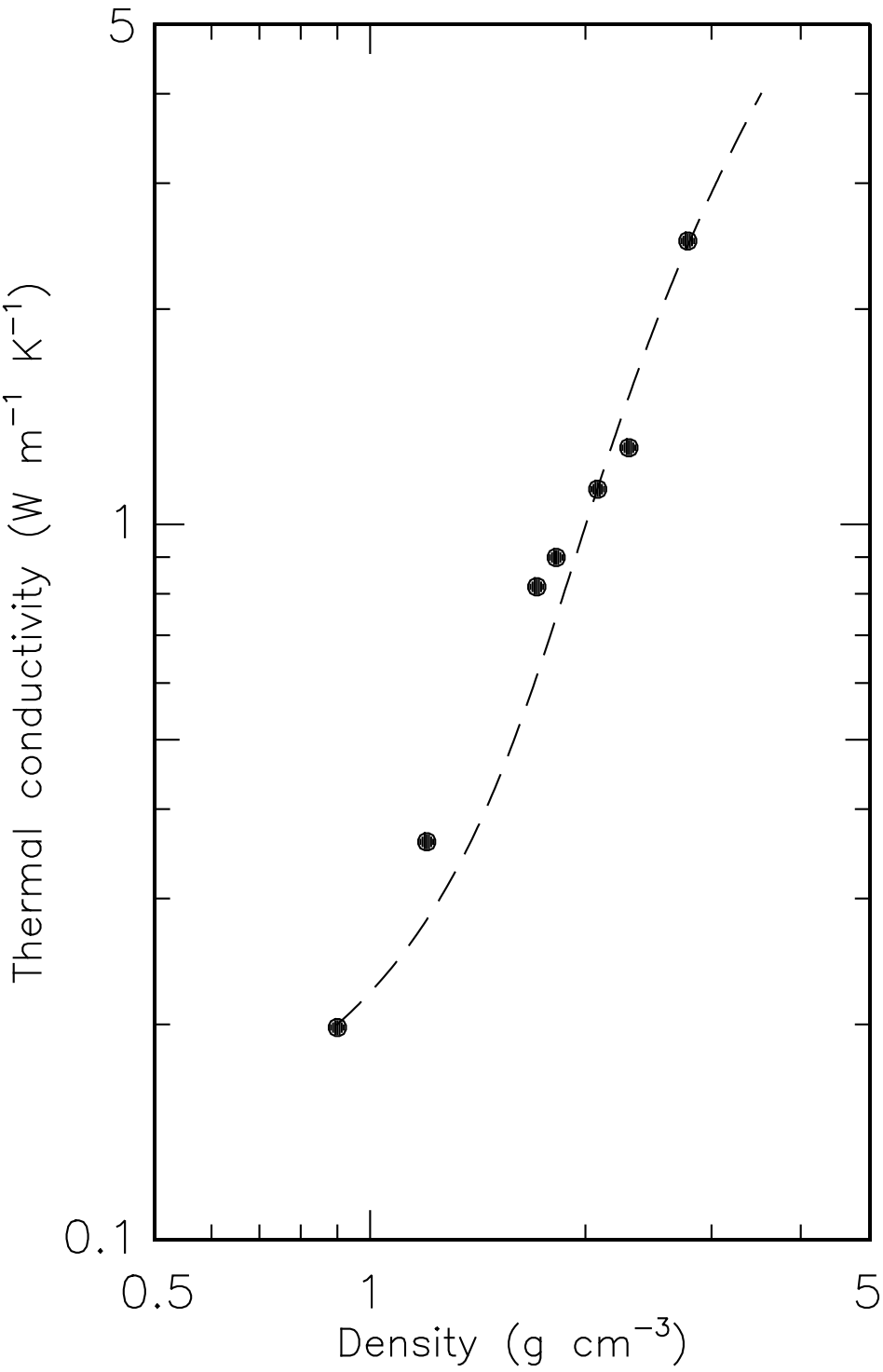

Figure 3

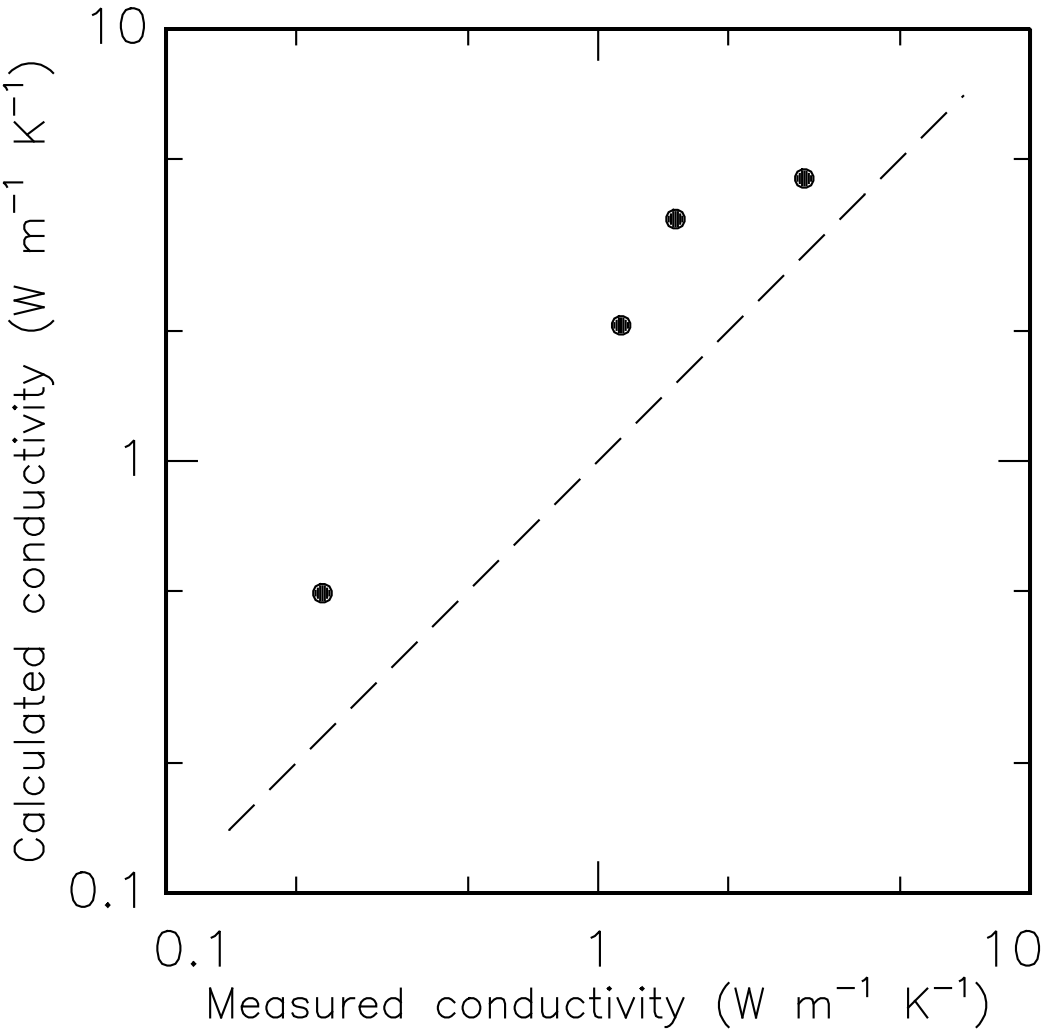
10
1
0.1
0.1
1
10
Calculated conductivity (W m^{-1} K^{-1})
Measured conductivity (W m^{-1} K^{-1})

Figure 4